Green Chemistry

Effects of thermal pretreatment and catalyst on biomass gasification efficiency and syngas composition

SCHOLARONE™
Manuscripts

Effects of thermal pretreatment and catalyst on biomass gasification efficiency and syngas composition

Singfoong Cheah[1,*], Whitney Jablonski[1], Jessica Olstad[1], Daniel Carpenter[1], Kevin Barthelemy[1], David Robichaud[1], Joy C. Andrews[2], Stuart Black[1], Marc Oddo[1], and Tyler L. Westover[3]

[1]National Renewable Energy Laboratory, 15013 Denver West Parkway, Golden, CO 80401

[2]Stanford Synchrotron Radiation Lightsource, SLAC National Accelerator Laboratory, 2575 Sand Hill Road, MS 69, Menlo Park, CA 94025

[3]Idaho National Laboratory, 2351 North Blvd, PO Box 1625, Idaho Falls, ID 83415-2025

*To whom correspondence should be addressed

Abstract

This work explores the combined effects of thermal pretreatment and using a catalyst *in-situ* on gasification carbon conversion efficiency, as well as product gas and tar content and compositions. To compare the effects of thermal pretreatment, pelletized and ground oak with three different levels of thermal pretreatment were gasified in a fluidized bed reactor. The pretreatments applied to the oak were (1) pelletization, (2) drying at 180 °C in air, and (3) torrefaction at 270 °C in nitrogen. The oak dried at 180 °C produced syngas of similar quality and approximately the same amount of char as untreated oak. Torrefaction at 270 °C resulted in syngas with a higher hydrogen to CO ratio, lower methane, and less than half of the total tar—all of which are desirable properties in terms of product gas quality. However, the oak torrefed at 270 °C also produced more than two times the amount of char as the untreated, pelletized oak. To determine the effect of catalyst, a series of experiments were conducted using olivine impregnated with nickel and cerium as the fluidized bed material in the gasifier. These tests showed that modified olivine can improve hydrogen production and reduce methane and tar levels in the syngas. The result was observed for both treated and untreated oak; although the effect was more substantial for untreated oak, for which the use of modified olivine reduced tar concentrations in the product gas by 60%, with a larger reduction in heavier tars than lighter tars. This result is important because reduction in heavier tar plays a more important role in benefitting downstream operations.

Keywords: gasification; biofuel; torrefaction; syngas; tar; olivine; reforming; indirect liquefaction; catalytic gasification

Introduction

Lignocellulosic-derived hydrocarbons are second-generation biofuels that have the potential to provide a substantial source of renewable fuels [1]. Biomass gasification to syngas and subsequent fuel synthesis is a promising route for competitive production of renewable fuels. Fisher-Tropsch synthesis had long been known as a process that can synthesize liquid fuels from

syngas [1, 2]. More recently, other high value fuel products such as synthetic natural gas [3], triptane [4-7] and other middle-distillate range molecules [8] have been targeted.

During the gasification process (also known as indirect liquefaction), secondary reactions produce tar and char that can impede downstream processing and decreases the fraction of carbon that is converted to useful syngas [9, 10]. The carbon yield to productive syngas has a significant effect on the economic viability of biofuels or bioproducts. In addition, the composition of the product gas generated during gasification is important as different fuel synthesis pathways may have specific H_2 to CO ratio requirements for the fuel synthesis catalyst to function effectively. Consequently, changes in feedstock treatment or the gasification process that produce a specific product gas composition and increase carbon yield can contribute to improvements in the biofuel economy.

It has been known that product gas composition can be controlled by the type of gasifier, fluidizing gas, and fluidized bed material. Gasifier configurations such as fixed bed, fluidized bed, entrained flow, and multi-stage each have different scalabilities, and can affect the biomass conversion efficiency as well as the amount of tar produced [11-13]. Fluidizing gas such as oxygen may lower the tar content of the product gas while water can increase hydrogen content of the product gas [14]. For fluidized bed material, adding active catalytic components such as nickel has been shown to decrease tars and hydrocarbons in the product gas [15-18]. The effect of certain biomass pretreatments, e.g., torrefaction, on gasification product gas, however, is less understood. To our knowledge, an investigation of the combined effect of catalytic gasification and torrefaction on product gas quality and carbon yield has not been conducted before.

Biomass torrefaction has been identified as a method to produce a feedstock that is less prone to rotting, has higher energy density, has lower transportation cost, and is easier to feed into a gasifier or pyrolyzer [19, 20]. During torrefaction, biomass is treated at a temperature typically higher than simple drying but less than that of pyrolysis in an inert atmosphere for 15 to 60 min. Bates et al. summarized torrefaction as typically occurring between 200 and 300 °C [21, 22]. After torrefaction, the biomass retains 80−95% of its original energy content and 70−90% of its mass while the remaining 10−30% of the biomass weight is released in the form of gaseous species [21]. Earlier research has shown that when torrefied between 230 to 300 °C, the gases/volatiles lost from wood consist primarily of water, acetic acid, carbon dioxide, methanol, and lactic acid [23]. Modeling of the weight and volatile loss kinetics suggests the volatile formation is primarily attributed to hemicellulose decomposition, with an increasing contribution of partial degradation of cellulose as temperature and reaction time increase [21].

Through thermodynamic analysis, Kuo et al. suggested that subsequent gasification of torrefied bamboo can produce higher syngas yield per kg of feed material because of the higher carbon content in torrefied bamboo [24]. Based on numerical modeling of the gasification of different feedstocks (raw biomass, torrefied biomass, and coal) in an entrained-flow reactor, Chen et al. concluded that the gasification performance of torrefied bamboo is enhanced compared to raw bamboo and is closer to that of bituminous coal [25]. Cerone et al. studied gasification of torrefied Eucalyptus and spruce in a fixed bed gasifier and found that the use of torrefied feed materials improved product syngas quality [26]. However, Horvat et al. recently reported that the use of torrefied *Miscanthus* x *giganteus* in a bubbling bed gasifier resulted in more tar formation than the unmodified feedstock [27]. These contradictory results indicate that more experimental data are needed to provide information to modelers and potential industrial applications. One of

the goals of this study is to determine the product gas quality and carbon conversion efficiency during gasification of torrefied biomass.

The inclusion of a catalytically active material in the gasifier itself has been shown to affect the syngas quality. Corella *et al.* hypothesized that though the mixing between the catalytic particles and the tar molecules in the gasifier may not be as effective as that in a downstream reformer because of the presence of other biomass particles, a catalyst inside the gasifier itself can be quite effective due to the catalytic conversion of "nascent," less refractory tars [28]. Indeed, research conducted with several different in-bed materials has shown improvements in carbon conversion efficiency and gas yields.

Garcia et al. studied the catalytic pyrolysis and gasification at 650 to 850 °C using nickel aluminate as in-bed material and reported high gas yield and carbon conversion with the catalyst in place [29-32]. Rapagna et al. examined olivine enriched with 10 wt.% Fe in a bubbling fluidized bed gasifier and found 60% and 40% reduction in tar and methane concentrations, respectively [33].   A study at the National Renewable Energy Laboratory using nickel-cerium-olivine for pyrolysis had shown 70% reduction in CH_4 and increased H_2 production [17], which might be related to nickel being a more effective methane reforming catalyst than Fe [34, 35], while ceria acts as a water gas shift catalyst [36]. More recent research investigated the effect of calcining on the stability of a modified olivine material [37], the deposition of coating on bed material [38], and the use of metal oxide modified bed material in a chemical looping mode [39, 40].

In this study, the combined effects of feedstock torrefaction and adding catalytic materials in the fluidized bed were investigated. This two-parameter study allowed us to evaluate and compare the effect of biomass and fluidized bed material modification, as well as to determine whether there is any combined or synergistic effect when both types of modifications are in place.

Materials and Methods

Feedstock Treatment and Characterization

The white oak used for the thermal pretreatment was obtained from Southern Kentucky Pellet Mill Inc. (Gamaliel KY, USA) as premium grade 100% bark less oak pellets. Three similar samples of pellets were prepared using a riffle splitter with riffles spaced at 25.4 mm. The first sample was not subjected to any further thermal pretreatment, though the pelletization process did include a 105 °C drying. The second sample was dried in air at 180 °C, and the third sample was torrefied at 270 ℃ in nitrogen. The thermal treatment system in which the drying and torrefaction were performed consists of horizontal auger-driven infeed and outfeed sections that connect to a vertical reactor. The reactor section is a 0.305 m diameter, 1.68 m tall stainless steel cylinder equipped with an agitation stirrer mechanism. The residence time of material in the heated reactor section was set to 30 minutes by controlling the feed rates in the infeed and outfeed augers. Details of the torrefaction equipment have been published previously [41]. After thermal treatment, the feedstocks were knife-milled and sieved to a size of 2 mm > x > 0.425 mm for gasification experiments. Since earlier research has shown that biomass particle size can affect mass and heat transfer during gasification [42], the use of small particle sizes (< 2mm) in our experiments ensured that the results would not be limited by mass and heat transfer.

During the actual gasification experiments, because we did not have sufficient quantity of the as-sieved white oak, a substitution from Country Boy White Lightning Pellet Fuel was used. This material is also of premium bark less grade. Proximate, ultimate, and ash analyses show that this white oak is practically the same as the one used in the 180 and 270 °C thermal treatment. This white oak was also sieved to a 2 mm > x > 0.425 mm size fraction.

Proximate analysis of the feed (moisture, volatiles, fixed carbon, and ash) was determined using a LECO TGA701 Thermogravimetric Analyzer. The carbon, hydrogen, and nitrogen contents of the untreated and torrefied oak were determined using a LECO TruSpec CHN module. Sulfur concentrations were determined using a LECO TruSpec Sulfur Add-On module.

Fluidized Bed Materials

The olivine used in the gasifier and for the catalyst preparation was supplied by AGSCO. Inductively coupled plasma analysis of the olivine indicates that there is 4.4% Fe and 0.25% Ni in the as-received material. The particle size distribution of the olivine is 80–1,000 μm, as determined with a Mastersizer 2000 particle size analyzer (Malvern Instruments), for which water was used as a dispersant in a Hydro 2000G accessory.

A nickel-cerium on olivine catalyst was synthesized using incipient wetness impregnation. The catalyst was prepared by drop-wise addition of a solution saturated in nickel and cerium nitrate to an olivine support. The salts used in the aqueous solution preparation are nickel (II) nitrate hexahydrate ($Ni(NO_3)_2 \cdot 6H_2O$) and cerium (III) nitrate hexahydrate ($Ce(NO_3)_3 \cdot 6H_2O$). The prepared catalyst was calcined at 450 °C for one hour followed by calcination at 800 °C for four hours in ambient air. Further details of the preparation method are available in Cheah *et al.* [17]. Inductively coupled plasma measurements of the prepared catalyst contained 2 wt.% Ni and 0.5 wt.% Ce.

The Ni-Ce Olivine catalysts were characterized using several methods, including X-ray Diffraction (XRD), Scanning Electron Microscopy (SEM), Energy Dispersive X-ray spectroscopy (EDS), and Transmission X-ray Microscopy (TXM). The TXM was conducted at beamline 6-2C at the Stanford Synchrotron Radiation Laboratory. TXM mapping at a spatial resolution of 30 nm was conducted above and below the Fe and Ni K-edges, and Ce L-edge. X-ray absorption spectroscopy was conducted although the data signals from each pixel (30 nm) were not of sufficient quality for species assignment.

Biomass Gasification

Biomass gasification experiments were carried out in a four inch (10.2 cm) inner diameter Inconel 800 reactor shown in Figure 1. The reactor is electrically heated and has a 6 inch (15.2 cm) freeboard for solids disengaging. Major components of the system are labeled with letters and include: biomass feeding system (A), fluidizing gas delivery (B), gasifier reactor (C), char knockout and collection (D), scrubber and condensate removal (E), and gas filtration and analytical systems (F).
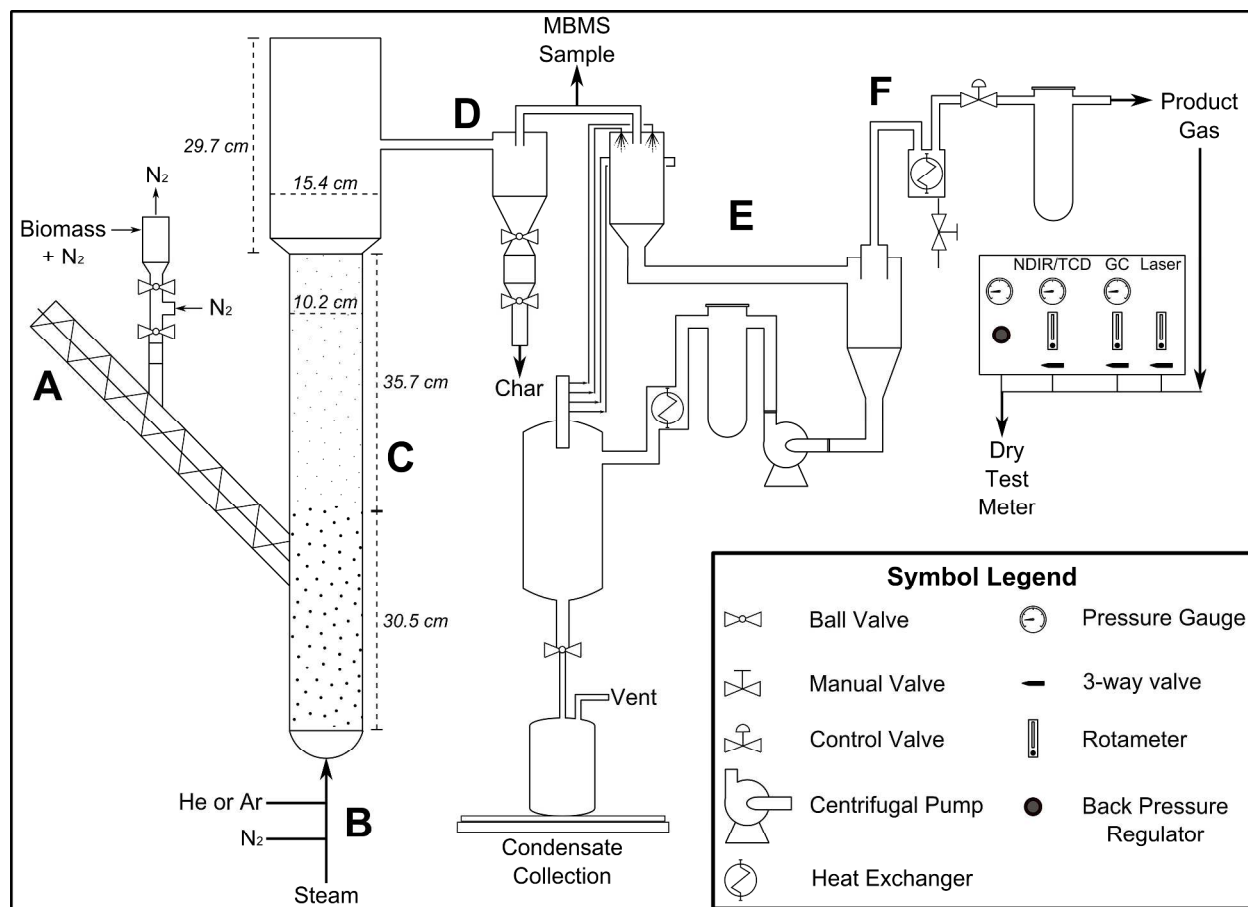
Figure 1. Schematic of the bench scale gasifier.

The feed system (A) consists of a loss-in-weight, dual screw solids feed hopper (K-Tron K2LT20), nitrogen (N_2) eductor, lock hopper type valve system, and jacketed feed auger. Biomass was loaded into the feed hopper and fed at 0.8 kg/hr into a funnel sitting atop the nitrogen eductor. The eductor is a nozzle fed with nitrogen (P = 650 kPa) that, when positioned below the funnel in a tube, creates a vacuum. Biomass was moved via this vacuum into the nitrogen stream flowing past the nozzle. This flowing nitrogen provided pneumatic transport of the biomass particles through a polyethylene tube to the cyclone at the top of the lock hopper. Nitrogen and biomass were separated in the cyclone, and nitrogen with entrained dust was returned to the feed hopper. Biomass particles sit at the base of the cyclone atop the first of two ball valves in the lock hopper system. These ball valves are separated by a 0.75 inch i.d. sanitary tee and an electrically actuated 2-way solenoid valve on the branch of the tee. Biomass was transported through the lock hopper system in a cycle:

1. Biomass dropped into a cyclone above the upper valve
2. Upper ball valve was opened
3. Solenoid valve with 80 kPa N_2 was opened (to break up biomass bridging)
4. Solenoid valve was closed
5. Upper ball valve was closed
6. Solenoid valve was opened and tee was pressurized with N_2

7. Lower ball valve was opened and biomass was charged onto the feed auger
8. Lower ball valve was closed

This cycle was repeated every 2.5 seconds. The feed auger is a 5/8" o.d. screw with flights separated by 5/8" pitch. The auger continuously carried biomass to the fluidized bed at a rate of 360 rpm. The purpose of the auger was to move the biomass from the lock hopper to the fluidized bed without exposing the bed to air. It is not meant to meter biomass at any specific rate. Biomass was metered using the feed hopper only.

Fluidizing gases (nitrogen, argon and/or super-heated steam, B) were fed to an Inconel coil heated to reaction temperature. These vapors and gases flowed to the base of the olivine bed through an Inconel gas distributor plate with 1/16" o.d. holes for gas transport. An electric boiler (Sussman MBA6F3) capable of producing 0.6 - 2 kg/hr steam was used, and the flow was measured by a Rosemount MFP orifice plate flow meter. In this set of experiments, the steam flow was 0.8 kg/hr, resulting in a steam to biomass ratio of 1:1. Teledyne-Hastings mass flow controllers were used to deliver nitrogen as well as helium (He) or argon (Ar) to the system. Steam and gases flowed through heated tubing (220 °C) to the base of the preheater coil.

During gasification, the preheater coil and reactor (C) were operated at 800 °C and the freeboard temperature was held constant at 700 °C. Outlet pressure was maintained between 25 – 30 kPa using a backpressure regulator on the analytical system to restrict gas flow. Three kilograms of industrial olivine, which resulted in 8 inch standing bed in the gasifier, was used as the fluidizing medium and steam was used as the fluidizing agent. Five thermocouples placed within the bed confirmed fluidization via uniform temperature (all points within 1 °C). Gas residence time in the reactor was calculated with the volume of the bed above the feed arm (not including the 8" standing bed) and half of the freeboard volume (where the product stream exits). Gas residence time at a fluidizing steam flow rate of 0.8 kg/hr at 800 °C and a reaction pressure of 30 kPa was calculated to be 8.6 seconds. If an approximate flow rate of 18.8 slm for syngas produced from 0.8 kg/h biomass in the reactor is added to the total flow through the reactor, the gas residence time is 6.9 seconds. This is probably a better approximation for the gas residence time because of the relatively large volume of gas produced instantaneously and continuously by biomass gasification.

Solids were removed in a heated cyclone (D) maintained at 400 °C and emptied into a heated knockout vessel. Solids then dropped by gravity through a ball valve on top of a cooling vessel, and were conveyed pneumatically into a char collection drum. Char was weighed at the end of each experiment, and the char production rate was approximated by dividing the total amount of carbon in the char collected by total gasification time. After solid separation, gas and vapors were quenched in a recirculating, cold (18 – 20 °C) dodecane scrubber system (E). Liquid and gas streams were separated with a cyclone separator. Tars and aerosols in the liquid stream were filtered using a 25 μm coalescing filter. A heat exchanger was used to cool gases, and gases were filtered in a 2 μm coalescing filter before the analytical equipment (F).

The product gas stream (F) was analyzed using a non-dispersive infrared (NDIR) gas analyzer tuned CO, CO_2, CH_4, and O_2 (California Analytical Instruments ZRE NDIR). Hydrogen (H_2) was measured continuously using a thermal conductivity detector (Nova 430SRM). Permanent gas speciation and quantification was achieved using an Agilent CP490 micro gas chromatograph (GC) equipped with three thermal conductivity (TCD) detectors. A mol-sieve 5Å (MS5A) column was used to separate and quantify helium, hydrogen, nitrogen, oxygen, methane

and carbon monoxide. A CP poraplot-Q (PPQ) column was used to separate and quantify carbon dioxide, ethylene, ethane, acetylene, propane, and propylene. A CP-sil 5 CB (5CB) column was used to separate and quantify 1-butene, 2-c-butene, and 2-t-butene.

Tar Measurements

Continuous, on-line chemical analysis of the hot process vapors was achieved using a molecular-beam mass spectrometer (MBMS). The MBMS instrument, developed at NREL, can be used to monitor a variety of thermochemical processes [43, 44]. It allows direct, real-time sampling of hot process gases and vapors, and provides a time-resolved account of the composition of the wet syngas. During gasification, this can be particularly useful in identifying and quantifying selected tar species in the gas.

For these tests, the product gas exiting the gasifier was routed to the MBMS sampling orifice through heated and insulated 1.28 cm (0.50") stainless steel transfer lines. A flow-through orifice sampling plate was used to continuously extract approximately 0.3 slm of the hot vapors for analysis, while the bulk of the gas (>20 slm) was routed back to the gasifier condensation system. The temperature of the tar sampling system, including the orifice plate, was maintained at 400 °C. This temperature was hot enough to prevent condensation losses in the sampling system, yet sufficiently cool to minimize further thermal decomposition of the tars being sampled.

Data collection and control of the mass spectrometer were automated using a PC-based data acquisition and control system manufactured by Extrel CMS. Mass spectra were recorded for m/z 30−400 at a rate of 1 scan/s, with 30-second averages stored. Mass spectral data were collected for each feedstock during periods of steady-state gasifier operation so that the composition and concentration of tar could be determined. During MBMS data collection, the inert tracer gas flow was switched from helium to argon to provide consistent reference signal intensity from run to run. The known mass flow of the tracer allowed conversion of tar concentration data to mass flow of individual compounds.

Absolute concentrations of selected tar compounds were determined by carefully controlled injections of a liquid calibration standard containing benzene, toluene, phenol, cresol, naphthalene and phenanthrene dissolved in methanol. The standards were metered in using an HPLC pump at rates of 0.25 or 0.50 mL/min through a heated capillary port upstream of the flow-through orifice plate. Additional details of the calibration procedure is in Carpenter et al. [44].

Laser Diode System

Hydrogen sulfide (H_2S) and ammonia (NH_3) in the product gas were detected using a diode laser spectrometer designed and built at NREL. The detection laser was setup in a multi-pass arrangement (Herriot cell) resulting in a 100 meter path length in a 0.5-meter long cell (~one liter in volume). Total pressure in the cell was maintained at 30 Torr, with no attempt to control temperature. Flow rate was approximately 11 slm dry gas (5 seconds residence time) and the signal was integrated over 3 seconds. The gas-phase H_2S and NH_3 absorption were detected at 6343.98 and 6528.89 cm^{-1} respectively using a fiber coupled diode laser tuned at those

frequencies. Detection was switched between NH_3 and H_2S using a fiber-switch. Prior to the start of the measurements, the absorption at those wavelengths were calibrated daily using 100 ppmv H_2S and 96 ppmv NH_3 standards. Detection limits were determined to be 2 ppmv for both gases.

Results

Feedstock Characterization

Solid yields, proximate and ultimate analyses for the untreated and torrefed oak are given in Table 1 and Table 2. Mass yield was calculated as

%Mass Yield = 100·solid product dry wt. / dry feedstock wt.   (Eq. 1)

Note that very little mass was lost due to drying at 180 °C, with a substantial reduction in moisture, indicating that volatilization of carbon-containing molecules is negligible at this temperature. With the 270 °C torrefaction, there was substantial mass loss, in agreement with existing scientific literature, which also contains detailed discussion of the types of molecules that are released at this temperature [21, 23, 45, 46].

The dried and torrefed oak samples had less moisture and a higher concentration of fixed carbon, indicating that the samples have been dried severely. The 180 °C sample had the same volatile content as the as-sieved oak, within experimental uncertainty. The volatile and fixed carbon content changed more dramatically when it was torrefed at 270 °C. The proximate analysis further reveals that with increasing torrefaction temperature, the oxygen concentration decreases and the carbon concentration increases. The higher carbon and lower oxygen concentrations result in a feedstock with higher energy density.

Table 1. Proximate analysis results (as-received basis) of the retained oak materials (material that passed through a 2.0 mm sieve and were retained on a 0.425 mm sieve). Note that in dry basis the volatile content of the 180 °C oak is less than that of the as-sieved material.

| Feedstock	Mass yield after treatment (%)	Proximate Analysis (wt. %)			
		Moistures	Volatiles	Fixed Carbon	Ash
Untreated		4.2 ± 1.1	83.4 ± 2.2	12.0 ± 1.2	0.4 ± 0.1
180 °C	98.7±0.3	1.5 ± 0.3	84.2 ± 1.4	14.0 ± 1.4	0.4 ± 0.1
270 °C	72.9±0.4	1.7 ± 0.3	78.9 ± 3.6	18.9 ± 3.4	0.5 ± 0.1

Table 2. Ultimate analysis results of the retained oak materials (material that passed through a 2.0 mm sieve and were retained on a 0.425 mm sieve).

| Feedstock | Ultimate Analysis (wt. %) | | | | | HHV |
	C	H	N	S	O[*]	(MJ/kg)
Untreated	48.1 ± 0.1	6.0 ± 0.6	0.09 ± 0.09	0.01 ± 0.0004	45.4	19.1
180 °C	49.4 ± 1.0	6.2 ± 0.0	0.05 ± 0.00	0.01 ± 0.002	43.9	20.0
270 °C	54.5 ± 0.9	6.0 ± 0.1	0.07 ± 0.01	0.01 ± 0.003	38.9	22.0

Values determined by taking the values of carbon, hydrogen, nitrogen, sulfur, and ash from unity. This O value does not include oxygen in water.

Scanning electron microscopy of the raw, torrefied oak were collected and compared to the biochar produced after gasification (Figure 2). SEM images of the Ni-Ce Olivine are available in an earlier publication [17]. A MiniSEM (Evex) was used to conduct the SEM analysis and to capture the surface structure images. A small amount of as-received biomass or biochar sample was mounted on carbon tape and gold coated using an Evex MSC-1000 Mini-Sputter Coater. The sample was observed under magnifications varying from 50x to 1,000x typically at 10 or 20 kV accelerating voltage.

The images show that untreated oak contains large particles with fibrous surfaces. The large particles observed are not surprising since the oak was sieved to 2 mm size fraction. After gasification, the biochar collected (far right in Figure 2) contained many small, fibrous-looking and slightly spongy particles. Some of the ultrafine particles observed might be ash or mineral particles. The larger particles, such as those in the untreated oak are no longer present. The oak torrefied at 270 °C has an intermediate appearance between the untreated oak and the biochar. It contains in general smaller particles, with fibrous surfaces and small particles deposited on the surfaces.


Untreated oak　　　　**Oak torrefied at 270 °C**　　　　**Biochar after gasification at 800 °C**
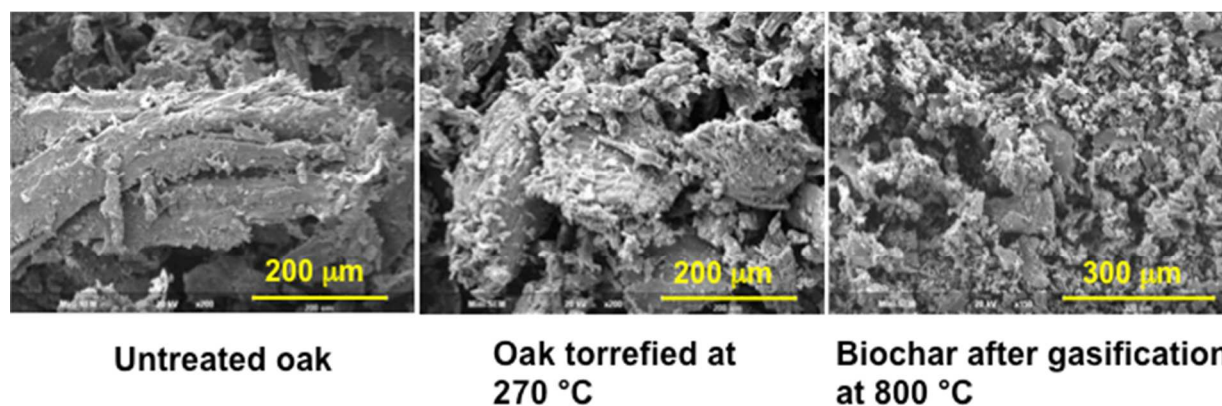
Figure 2. SEM images of the raw oak, oak torrefied at 270 °C, and a biochar after gasification at 800 °C.

Product gas composition

The experiments were generally conducted in 8 to 10 hours, although the measurements were typically acquired for the first 7 to 8 hours only. Figure S1 in the supporting information shows the number of moles of H_2 produced as a function of time and also serves to show the time dependence of the gases produced. For all the conditions, the number of moles of H_2 produced approached steady state in approximately 1.4 to 3 hours and was quite stable from that point onwards. Any deactivation of the Ni-Ce Olivine catalyst primarily occurred within the first two hours, where the number of moles of H_2 produced decreased with time. The number of moles of H_2 produced using the plain olivine increased with time. A discussion of this time dependence is presented in the Discussion section (under the subsection *Catalytic Gasification*).

At approximately the 3rd to the 5th hour, the helium tracer was switched to argon tracer to allow for MBMS measurements of the tar speciation. Note that the data for light gases (in percent volume of gas) were measured during the entire experiment (duration 7-8 hours). However, because the GC-MS analyzes helium but not argon, the actual number of moles of the different gases produced (which requires data on the volume of gases produced as well as the gas composition measured by GC-MS) was only available when the helium tracer was on. The near steady state data (with absolute value change <4%) for the light gases that were produced, typically averaged over the time scale of 5th to the 7th hour, were used in the mass balance calculations and are presented in the bar plots presented in Figures 3−5.

The H_2 concentrations in the product gas are shown in Figure 3. Within experimental uncertainties, the H_2 concentrations produced from untreated oak and 180 °C dried oak were similar. The 270 °C torrefied oak produced a gas that was richer in H_2 than the other two feed materials. For every feedstock, it can be seen that the use of Ni-Ce Olivine consistently produced a gas with higher H_2 concentrations. The reason for this increase will be discussed in the Discussion section.
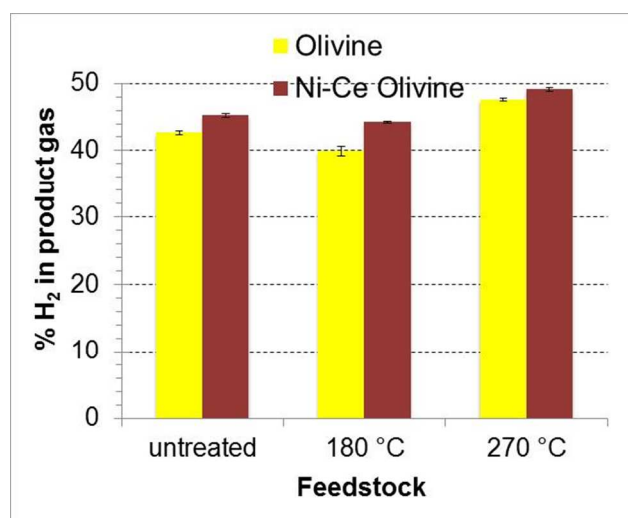

Figure 3. H_2 concentrations in the product gas for the three feedstocks and the two fluidized bed materials used in this study. The uncertainty bars represent the standard deviation of the gas phase H_2 values during the time period of data.

Green Chemistry

The steady state gas phase H_2/CO results are shown in Figure 4. The uncertainty bars represent the standard deviation of the gas phase H_2/CO values during the time period of data. The results show that with the exception of the feedstocks torrefied at 270 °C, the H_2/CO ratio was approximately 1.5 for all samples. Using the 270 °C torrefied oak results in H_2/CO of approximately 1.8, which can be advantageous for certain applications. In our earlier research, we found that modified olivine had a significant effect in increasing the H_2/CO ratio when steam was absent. In this study, where the steam to biomass ratio is 1:1, the use of modified olivine had a more minor effect on H_2/CO ratio, though its effect was more significant for the untreated and 180 °C dried materials.
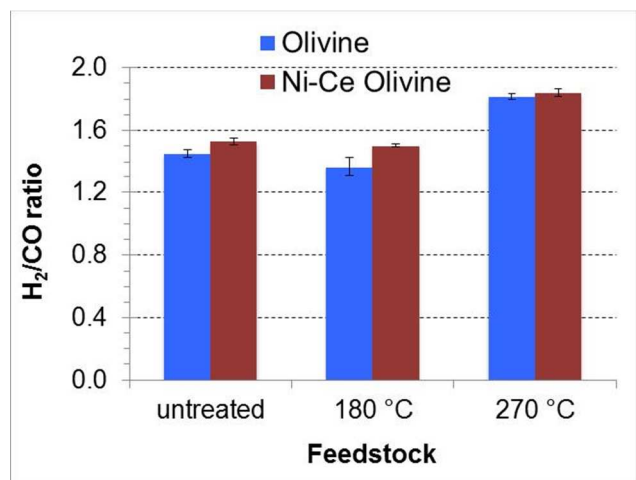
Figure 4. The steady state H_2/CO ratio under various experimental conditions.

The steady state gas phase CH_4 results are shown in Figure 5. The uncertainty bars represent the standard deviation of the gas phase CH_4 values during the time period of data. The results show that for untreated and 180 °C dried oak, the gas phase methane was 9.0−9.6 %. Using the Ni-Ce Olivine bed material reduced the gas phase CH_4 by 2% in both cases. Using the 270 °C torrefied oak with unmodified olivine decreased the gas phase CH_4 to approximately 7.3 ± 0.1 %. This suggests either the use of a catalytically active bed material or torrefied feedstock can reduce the methane levels in the product gas. With a combination of both Ni-Ce Olivine bed material and oak torrefied at 270 °C, the gas phase CH_4 was 6.4 ± 0.1 %.
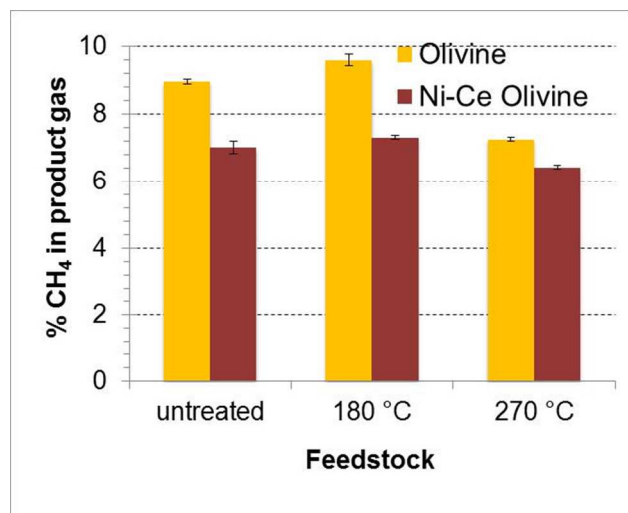
Figure 5. Percent methane in dry, inert free basis in the product gas as a function of conditions.

The gas phase NH_3 and H_2S were measured using a diode laser system. Within the uncertainty of the diode laser measurements, there was no difference between the gas phase NH_3 and H_2S levels when untreated and torrefied oak were gasified. All of the different conditions produced a gas phase NH_3 and H_2S of 170 ± 50 and 20 ± 10 ppmv, respectively.
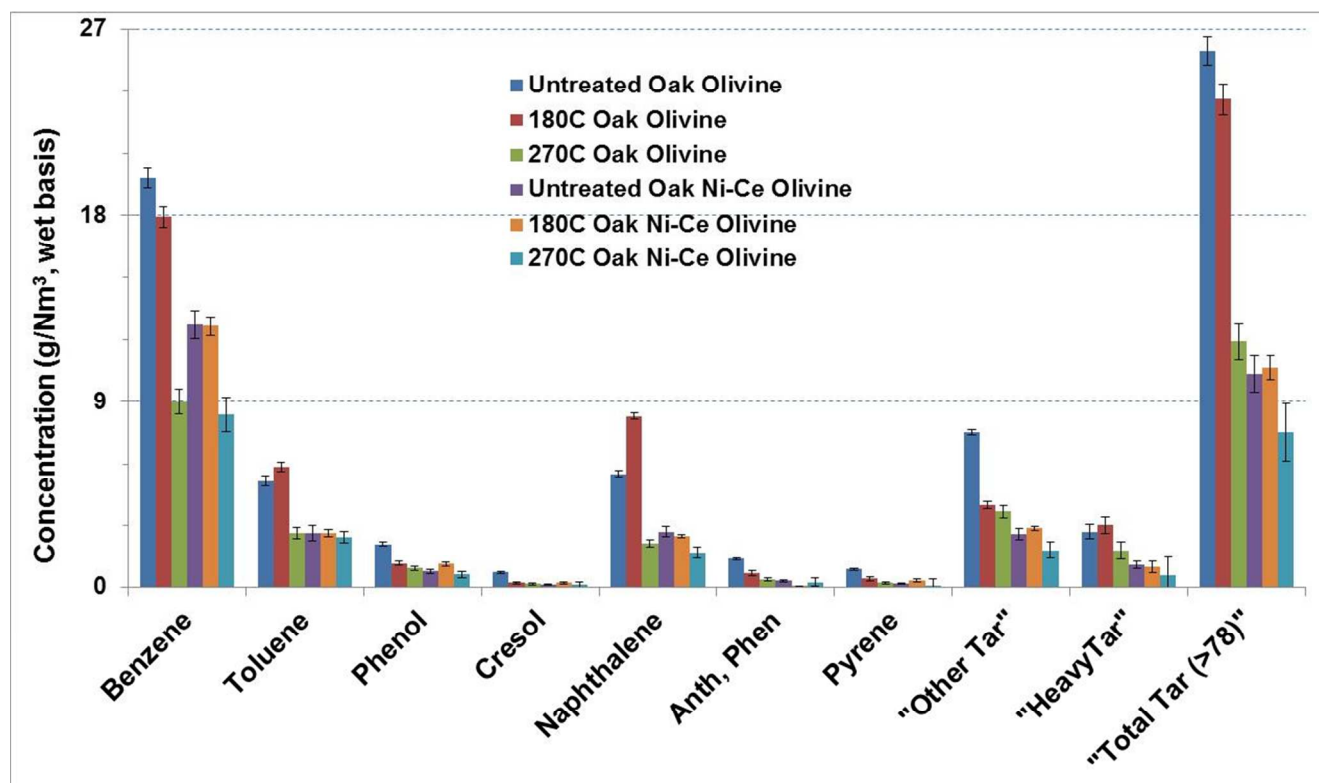
Tar Speciation

The concentrations of the different tar species were determined by collecting and analyzing MBMS spectra of the hot gas components. Figure 6 shows the concentrations of major tar species measured in the raw syngas, determined using the peak intensity at the corresponding AMU (toluene, 92; phenol, 94; cresol, 108; naphthalene, 128; pyrene, 202). The AMU 178 peak is attributable to either anthracene or phenanthrene. The "other tar" included summations of mass spectral peaks AMU 80−176 using the response factor calculated from 128, which was obtained with a standard. The "heavy tar" is the summation of mass spectral peaks 180-400, using the response factor calculated from 178. The uncertainties ($\pm 2s$) were estimated from the standard deviations of the average signal during each steady-state measurement period.

The European Committee for Standardization (CEN) defines "tar" as "all organic compounds present in the gasification product gas excluding gaseous hydrocarbons (C1 through C6)" [47]. Another "operational" definition of tar is organic compounds that condense and cause problems in the condenser and transfer lines [9]. Under both definitions, benzene (boiling point 80.1 °C) is normally not considered a tar or included in "total tar" calculations. Because of the low boiling point of benzene, it is also not captured by traditional sampling methods such as impinger or condensation methods. The "total tar (>78)" in Figure 6 corresponds to what is generally presented as "total tar" in the literature. The data for benzene (AMU 78) is also presented in Figure 6 as additional/bonus information since the MBMS allowed us to measure the gas composition at 400 °C and because the concentration of benzene can be useful information (it is either considered carbon loss as it is not part of the synthesis gas or potentially can be separated as a commodity chemical).

The untreated oak gasified with unmodified olivine produced the highest amount of total tar (26 g/Nm^3 wet basis and 46 g/Nm^3 dry basis) and the highest amount of the major species including benzene, phenol, cresol, anthracene, pyrene, and "other" tars. Using oak dried at 180 °C with the same unmodified olivine resulted in the oxygnenated species such as phenol, cresol, and "other tar" decreased by almost half. However, the hydrocarbon type tars such as benzene, toluene, and "heavy tar" showed no reduction; the amount of naphthalene actually increased when the 180 °C torrefied oak was used.

Using oak torrefied at 270 °C with the unmodified olivine, the total tar concentration decreased by more than half (12 g/Nm^3 compared to the baseline of 26 g/Nm^3, both values in wet basis). The reduction in tar levels was more substantial for oxygenate and light hydrocarbon species such as benzene (a 55% reduction) than for heavy tars (a 35% reduction).

When Ni-Ce Olivine was used, the total tar concentrations decreased for every feedstock. The reduction in heavier tar (toluene and up) was more substantial than that for lighter tar such as benzene. This trend was observed for every feedstock. Since the heavier tars are more problematic in terms of causing downstream plugging type problems, this result is an important consideration on the future potential of catalytic gasification.

Figure 6. Concentration of benzene and major tar species measured in the raw syngas for the three feedstocks with olivine or nickel-cerium modified olivine.

Carbon conversion efficiency

Figure 7 shows the fraction of carbon in light gas, which was calculated by dividing the carbon content of the light gas produced by the carbon input to the gasifier. The light gas produced was obtained by summing the number of moles of carbon in the light gases measured, which are CO, CO2, methane, ethylene, acetylene, propylene, propane, 1-butene, and 2-butene. The molar mass flow of the gases produced was calculated using helium as a tracer gas. Using the 270 °C material resulted in quite a substantial reduction in overall carbon efficiency, while the use of catalytic gasification improves carbon conversion to light gas.

Figure 8 shows the fraction of biomass carbon being partitioned to tar. Overall, torrefaction had a larger positive effect on the carbon fraction converted to tar. However, as indicated in the tar speciation section, catalytic gasification had a more significant effect in reducing the heavy tar fraction and consequently the fraction of carbon being converted to heavy tar was also less.

Figure 9 shows the fraction of carbon converted to biochar under different conditions. In both olivine and Ni-Ce Olivine cases, the oak torrefied at 270 °C had twice as much of its carbon in the form of char as the untreated or more mildly treated oak, an increase that was statistically significant. The use of Ni-Ce Olivine had no effect on the fraction of carbon converted to biochar for each feedstock.
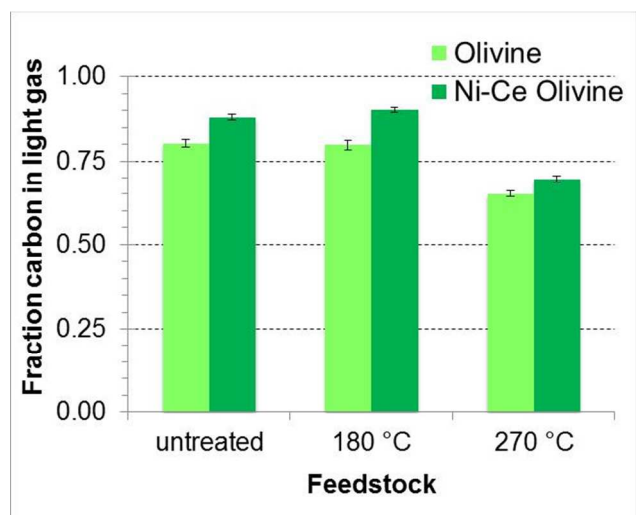

Figure 7. Fraction of carbon in light gas produced under different experimental conditions
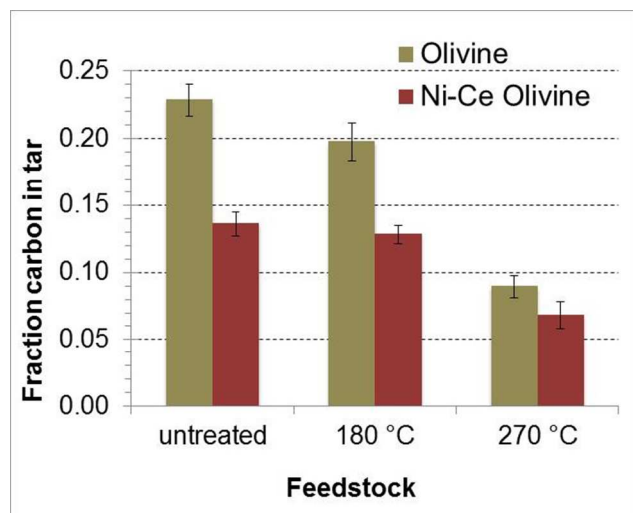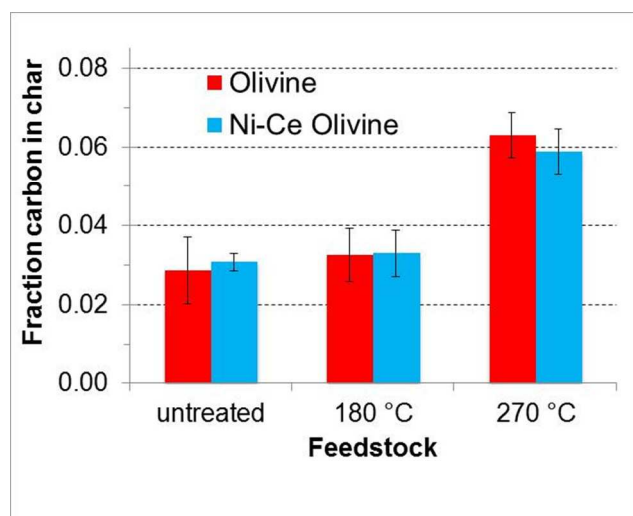
Figure 8. Fraction of biomass carbon partitioned to tar under different experimental conditions.


Figure 9. Fraction of carbon in the biomass being converted into biochar under different experimental conditions. The uncertainty of the measurements was obtained from calculating standard deviation of the repeat runs, which were performed for three out of the six conditions. Where no repeat run was conducted, the uncertainty was the average of the three standard deviations described above.

Table S1 shows numerical data for the fraction of carbon among different phases during the thermal treatment and the gasification process, which partitioned the biomass fed into the gasifier into light gas, tar, and char. The carbon in each fraction was independently measured and the equations are presented below Table S1.

Pre- and post- reaction fluidized bed material

X-ray Diffraction of the as-received olivine shows that the material is primarily forsterite, a magnesium silicate (Mg_2SiO_4). The as-prepared Ni-Ce Olivine shows XRD lines dominated by forsterite with additional line contributions from nickel oxide and cerium oxide (Figure S2). In our earlier SEM-EDS measurements of the catalyst, the nickel appears as a surface coating and iron was not detected with EDS. Using the TXM method, which has a much higher spatial resolution and can penetrate deeper into the sample, we were able to determine that the nickel oxide exists as "islands" of particles on the olivine (Figure 10).
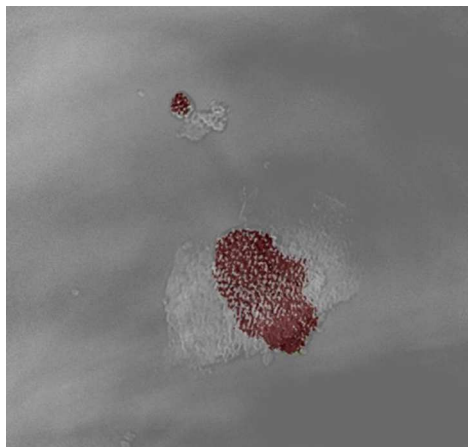
Figure 10. TXM image of the distribution of Ni and Fe on the Ni-Ce Olivine particle at a spatial resolution of 30 nm; the red color is Ni, while the light gray color is Fe. The signal from Ce was too weak.

In our earlier research on the effect of Ni-Ce Olivine on biomass pyrolysis (or gasification in nitrogen only), XRD evidence for Ni metal was found after pyrolysis [17]. In the XRD examination of the Ni-Ce Olivine after gasification (in the steam environment used in the current research), the lines for NiO decreased in intensity but did not completely disappear (Figure S2). There were several XRD lines that could indicate formation of iron-nickel or other alloys but no definitive lines for metallic nickel. This may be because the reduction of NiO in a steam environment could be slower than in a dry gas environment, as a high steam environment could lead to lower coverage of H_2 on the catalyst, which has been shown to be less favorable to NiO reduction [48].

A measure of the nickel and cerium content in the char collected after gasification provides an estimate of nickel and cerium loss from the fluidized bed material. Based on those measurements, we determined that 10–16 % of the nickel and cerium was lost after 8 hours in a fluidizing environment.

Discussion

Comparison of Results with the Literature

Table S1 and Figures 7, 8, and 9 show the fraction of carbon in various phases. Out of the components of the light gases, CO is particularly important since H_2 and CO are the main components used for liquid fuels and bioproduct synthesis (with the exception of the use or development of catalysts that are effective in incorporating CO_2). The CO efficiency, which is

16

defined as the number of moles of CO formed per mole of carbon in the feedstock, is often used in comparison of the effectiveness of gasification operation. Using untreated oak and as-received olivine, our CO efficiency is 0.39, a value that compares favorably with CO efficiency in the literature [49, 50], which ranges from 0.2 to 0.4.

In the literature of biomass gasification, it has been shown that tar levels can vary by as much as two orders of magnitude [9]. The wide range of tar reported is not just a function of the different gasifier configuration or fluidizing gases, but also reflects the different sampling methods [9]. The MBMS method used in this research had been quantitatively measured against traditional impinger sampling method and was shown to be within 6% of the known method [44].

Using unmodified olivine and untreated oak, our measurements of 26 g/Nm^3 total tar in wet basis or 46 g/Nm^3 in dry basis is within the typical range of tar concentrations reported in the literature, e.g., 2.2–42 g/Nm^3 (dry basis) reported by Perez et al. [51] and the 2–100 g/Nm^3 range for fluidized bed gasifiers in Table 3.I. of Milne et al. [9].

Catalytic Gasification

A large number of reactions occur in the gasifier, including particle level devolatilization, cracking, and reforming [12, 13]. Because the relative kinetics of these reactions affect the resultant gas composition and optimization of gasifier design, a number of different research groups have conducted extensive modeling on these reactions [52, 53]. For example, Stark et al. used a reaction network model to model an air-blown gasifier and were able to predict the concentrations of many gases reliably, except for CO oxidation kinetics and the concentrations of polyaromatic hydrocarbons [52]. The previous modeling also concluded that a radical growth pathway likely played a central role in the growth of PAH [52]. Our hypothesis is that the modified olivine surface is more effective in impeding the growth of the heavier tar species or that it reforms the heavy tars already formed [17], just as a downstream tar-reforming catalyst would.

The use of Ni-Ce Olivine as a fluidized bed material also affects the light gas composition: the H_2 concentration and the H_2/CO ratio both increased with a concomitant decrease in the CH_4 and tar concentrations. These trends were observed for every feedstock. The steam reforming reactions of tar and methane are shown below [54].

$$C_nH_m + nH_2O \rightarrow nCO + (n + \tfrac{1}{2} m) H_2 \qquad \Delta H_{298°} = 1175 \text{ kJ/mol for } n = 7, m = 16 \qquad (1)$$

$$CH_4 + H_2O \rightarrow CO + 3H_2 \qquad \Delta H_{298°} = 206 \text{ kJ/mol} \qquad (2)$$

The stoichiometry of the reforming reactions would suggest that for each mole of CH_4 consumed, there should be one mole of CO and three moles of H_2 produced. When Ni-Ce catalyst was used, the actual increase in number of moles H_2 produced was more than three times of the decrease in CH_4 compared to plain olivine. This may be attributed to H_2 produced from tar reforming.

As shown in Figure S1, during the first 1.5 hours the production of H_2 decreased for all three feedstocks with Ni-Ce Olivine as the bed material. We hypothesize that a fraction of fine nickel and cerium particles could be rapidly reduced *in situ*, resulting in the larger amount of H_2 produced early on. However, these fine particles were easily lost during the first 1.5 hours, resulting in decreased H_2 production. There was nevertheless stable Ni and Ce on the catalyst

surface to retain an improved performance over plain olivine during the entire measurement period, a conclusion that that was supported by the finding of only 10–16% Ni and Ce loss. Future tests would be necessary to determine material robustness over longer term and whether a glass ceramic material [55, 56] might be a potential solution.

Starting from the 2nd hour, the slow increase in total H_2 produced over time (Figure S1) may be because as time passed less H_2 was consumed for reduction of the catalyst. Overall, more H_2 and higher carbon conversion efficiency were obtained with the Ni-Ce Olivine catalyst, so the consumption of H_2 in catalyst reduction, if any, did not result in lower performance.

For plain olivine, with all three feedstocks, there was a slow increase in H_2 production during the entire measurement period. This may be related to slow reduction of iron in the olivine in the absence of nickel. Future high quality TXM studies of the catalyst may provide more information on the catalyst reduction and the mechanism of modified olivine in reducing tar content of the syngas.

Torrefaction

The syngas generated from oak torrefied at 270 °C has higher H_2/CO content, less than half the tar, and 20% less methane than the syngas produced from untreated oak, which makes the syngas generated from the torrefied oak superior in quality. However, the 270 °C torrefied material had 6% of its carbon converted to char, as compared to 3% for the untreated oak.

It is known that lignin condensation reactions can occur during the heating of wood [57, 58]. In addition, because the torrefaction process removes the fraction of more loosely bound carbon molecules that were likely fragments of a larger polymer, e.g., acetic acid derived from hemicellulose [19], the materials left behind such as the cellulose and lignin polymers are more recalcitrant and may be more challenging to gasify. Viewed in this regard, it is not surprising that gasification of torrefied feedstocks produced more char and fewer volatiles, including tar. It should be noted that a recent study indicates oak may behave differently at 300 °C and loses more lignin than cellulose and hemicellulose [59]. However, it is not clear whether that conclusion applies to our feedstock, which was torrefied at 270 °C since mass and compositional changes are particularly large as the torrefaction temperature reaches 300 °C [46].

It is less clear why the use of torrefied and dried materials had more influence on decreasing lighter tars (for the 270 °C torrefied oak) or oxygenates (for the 180 °C dried oak). It has been theorized that biomass devolatizes readily to form pyrolysis vapors, which then form CO and H_2 or C_{2-5} radicals that subsequently form polyaromatic hydrocarbons (PAH) [17, 60]. Since torrefaction of beech [46] and willow [23] have been shown to selectively remove hemicellulose and cellulose, it can be surmised that primary pyrolysis products normally associated with hemicellulose and cellulose may be present in the torrefied feedstock at lower concentrations than whole oak [46]. This in turn could lead to lower total tar and a different distribution of tar species.

Our findings of reduced tar content is different from that of Horvat et al., where the use of torrefied *Miscanthus* x *giganteus* increased tar levels in the syngas [27]. The difference might be related to differences during the torrefaction, e.g., the fixed carbon content of oak increased from 12.0 to 18.9 % after the 270 °C treatment we used (Table 1), while the fixed carbon content of

Miscanthus x *giganteus* increased from 10.7 to 23.9 % after the torrefaction procedure used in the Horvat *et al.* [27] study. The higher fixed carbon content of the torrefied *Miscanthus* x *giganteus* might have contributed to the higher tar concentrations measured.

Process and gasifier optimization

Overall, from a process perspective, both the reduction in tar concentration and the reduction in the fraction of carbon being converted to tars are encouraging. The actual concentration of tar tolerated depends on the downstream applications [9], though in general it is accepted that the maximum tar levels should not be more than 60–600 mg/Nm^3 [9]. Based on this criterion, our lowest achieved tar concentration of 7,000 mg/Nm^3 on a wet basis (using the 270 °C torrefied feedstock with Ni-Ce Olivine bed material) is currently not substantial enough to eliminate the need for a downstream cleanup step, e.g. a reformer. We have also recently discovered that the mixing between the fluidizing medium and the feedstock may not have been optimal in this reactor, indicating that the effect of the catalyst will likely be more substantial with an improved reactor design.

When the gasifier was designed and built [42], it was assumed that the entrance point of the biomass feed into the gasifier facilitated good back mixing between the biomass particles and the bubbling fluidized bed (BFB) to maximize heat transfer and gasification. Subsequent computational fluid dynamics (CFD) modeling done in conjunction with the Reaction Gas Dynamics (RGD) laboratory at Massachusetts Institute of Technology (MIT) elucidated aspects of the system that suggest that the top of the BFB is 6 inches lower than originally assumed and that there was not adequate mixing between the catalyst bed and the biomass particles [53]. It is likely that some of the catalyst interacted with biomass particles near the top of the BFB though the entire catalyst bed was not engaged effectively. The observed catalyst activity would have been lower than expected based on predictions because the residence time and extent of reactants mixing with the catalyst would be difficult to determine. Though this results in an underutilization of the catalyst material and higher than expected tar and methane levels when a catalyst was used in the gasifier, each fluidizing material will have contacted the biomass particles in the same way. Therefore, the results presented in this study demonstrate accurate relative comparisons between nickel-cerium-doped and unmodified olivine catalysts. Our results indicate that to fully utilize a catalyst in a gasifier, the gasifier needs to be designed to maximize mixing. The modification is currently being conducted at NREL.

To make the gasification of torrefied material more economical, a recycle or carbon capture step during the torrefaction process can help conserve additional carbon. The use of torrefied materials may also require different gasification process parameters. For example, the 270 °C torrefied oak generates syngas of high quality though at the expense of a large fraction of carbon being converted to char, thus an investigation on whether gasification at a higher temperature could decrease the carbon remaining in char may be warranted. It has been reported that higher temperature gasification can produce more recalcitrant tars [9] so the tar distribution has to be measured and a decision on operational parameters be carefully balanced between carbon conversion to char vs. recalcitrant tars. A secondary combustor to fully utilize the high carbon fraction in char may be a possible technological solution.

Conclusions

Our results show that both torrefaction and the use of a catalytically active bed material can improve the syngas quality from fluidized bed gasification. Using a catalytically active material is quite appealing as it increases the fraction of biomass/carbon going to useful products and reduces heavy tars in the syngas without increasing the fraction of carbon being converted to char. The life and regenerability of the catalyst would need to be evaluated in such a case. To improve on the overall process, the gasifier must be designed for good mixing between the biomass material and the fluidizing medium.

Using torrefied feedstock can result in improved syngas quality, although significantly more of the carbon fraction was being converted into char. This, in addition to the carbon loss during the torrefaction process itself, lowers the economic appeal of this process. A process that captures the carbon during the torrefaction stage can potentially improve the carbon efficiency and the economics, although it does increase process complexity. A full evaluation of the process economics will need to be undertaken.

Acknowledgments

References

[1] R.P. Anex, A. Aden, F.K. Kazi, J. Fortman, R.M. Swanson, M.M. Wright, J.A. Satrio, R.C. Brown, D.E. Daugaard, A. Platon, G. Kothandaraman, D.D. Hsu, A. Dutta, Techno-economic comparison of biomass-to-transportation fuels via pyrolysis, gasification, and biochemical pathways, Fuel, 89 (2010) S29–S35.
[2] T. Damartzis, A. Zabaniotou, Thermochemical conversion of biomass to second generation biofuels through integrated process design—A review, Renewable and Sustainable Energy Reviews, 15 (2011) 366–378.
[3] M. Gassner, F. Marechal, Thermo-economic optimisation of the polygeneration of synthetic natural gas (SNG), power and heat from lignocellulosic biomass by gasification and methanation, Energy & Environmental Science, 5 (2012) 5768–5789.
[4] J.H. Ahn, B. Temel, E. Iglesia, Selective homologation routes to 2,2,3-trimethylbutane on solid acids, Angewandte Chemie International Edition, 48 (2009) 3814–3816.
[5] J.E. Bercaw, P.L. Diaconescu, R.H. Grubbs, R.D. Kay, S. Kitching, J.A. Labinger, X. Li, P. Mehrkhodavandi, G.E. Morris, G.J. Sunley, P. Vagner, On the mechanism of the conversion of methanol to 2,2,3-trimethylbutane (triptane) over zinc iodide, The Journal of Organic Chemistry, 71 (2006) 8907–8917.
[6] N. Hazari, E. Iglesia, J.A. Labinger, D.A. Simonetti, Selective homogeneous and heterogeneous catalytic conversion of methanol/dimethyl ether to triptane, Accounts of Chemical Research, 45 (2012) 653–662.
[7] J.A. Schaidle, D.A. Ruddy, S.E. Habas, M. Pan, G.H. Zhang, J.T. Miller, J.E. Hensley, Conversion of dimethyl ether to 2,2,3-trimethylbutane over a Cu/BEA catalyst: Role of Cu sites in hydrogen incorporation, Acs Catalysis, 5 (2015) 1794–1803.

[8] M. Behl, J.A. Schaidle, E. Christensen, J.E. Hensley, Synthetic middle-distillate-range hydrocarbons via catalytic dimerization of branched C_6–C_8 olefins derived from renewable dimethyl ether, Energy and Fuels, 29 (2015) 60786087.

[9] T.A. Milne, R.J. Evans, N. Abatzoglou, Biomass gasifier tars: their nature, formation, and conversion, National Renewable Energy Laboratory, Golden, CO, 1998, pp. 204 pp.

[10] J. Corella, J.M. Toledo, G. Molina, A review on dual fluidized-bed biomass gasifiers, Ind. Eng. Chem. Res., 46 (2007) 6831−6839.

[11] C. Higman, M. van der Burgt, Gasification, 2nd ed., Gulf Professional Publishing, an imprint of Elsevier, Burlington, MA, 2008.

[12] P. Basu, Biomass Gasification and Pyrolysi: Practical Design, Academic Press2010.

[13] V.S. Sikarwar, M. Zhao, P. Clough, J. Yao, X. Zhong, M.Z. Memon, N. Shah, E.J. Anthony, P.S. Fennell, An overview of advances in biomass gasification, Energy & Environmental Science, (2016).

[14] J. Gil, J. Corella, M.P. Aznar, M.A. Caballero, Biomass gasification in atmospheric and bubbling fluidized bed: Effect of the type of gasifying agent on the product distribution, Biomass and Bioenergy, 17 (1999) 389–403.

[15] J. Arauzo, D. Radlein, J. Piskorz, D.S. Scott, New catalysts for the fluid bed catalytic gasification of biomass, in: A.V. Bridgwater (Ed.) Advances in Thermochemical Biomass Conversion, Blackie Academic & Professional, London, 1994, pp. 201−215.

[16] L. Garcia, M.L. Salvador, J. Arauzo, R. Bilbao, Steam gasification of biomass in fluidized bed using a Ni-Al coprecipitated catalyst, in: R.P. Overend, E. Chornet (Eds.) Making a Business from Biomass in Energy, Environment Chemicals, Fibers, and Materials, Elsevier Science, Oxford, U.K., 1997, pp. 373–382.

[17] S. Cheah, K.R. Gaston, Y.O. Parent, M.W. Jarvis, T.B. Vinzant, K.M. Smith, N.E. Thornburg, M.R. Nimlos, K.A. Magrini-Bair, Nickel cerium olivine catalyst for catalytic gasification of biomass, Applied Catalysis B: Environmental, 134–135 (2013) 34–45.

[18] S. Rapagna, N. Jand, P.U. Foscolo, Catalytic gasification of biomass to produce hydrogen rich gas, International Journal of Hydrogen Energy, 23 (1998) 551–557.

[19] M.J.C. van der Stelt, H. Gerhauser, J.H.A. Kiel, K.J. Ptasinski, Biomass upgrading by torrefaction for the production of biofuels: A review, Biomass and Bioenergy, 35 (2011) 3748–3762.

[20] T.C. Acharjee, C.J. Coronella, V.R. Vasquez, Effect of thermal pretreatment on equilibrium moisture content of lignocellulosic biomass, Bioresour. Technol., 102 (2011) 4849–4854.

[21] R.B. Bates, A.F. Ghoniem, Biomass torrefaction: Modeling of volatile and solid product evolution kinetics, Bioresour. Technol., 124 (2012) 460–469.

[22] R.B. Bates, A.F. Ghoniem, Modeling kinetics-transport interactions during biomass torrefaction: The effects of temperature, particle size, and moisture content, Fuel, 137 (2014) 216–229.

[23] M.J. Prins, K.J. Ptasinski, F. Janssen, Torrefaction of wood - Part 2. Analysis of products, Journal of Analytical and Applied Pyrolysis, 77 (2006) 35–40.

[24] P.-C. Kuo, W. Wu, W.-H. Chen, Gasification performances of raw and torrefied biomass in a downdraft fixed bed gasifier using thermodynamic analysis, Fuel, 117 (2014) 1231–1241.

[25] W.-H. Chen, C.-J. Chen, C.-I. Hung, C.-H. Shen, H.-W. Hsu, A comparison of gasification phenomena among raw biomass, torrefied biomass and coal in an entrained-flow reactor, Applied Energy, 112 (2013) 421–430.

[26] N. Cerone, F. Zimbardi, A. Villone, N. Strjiugas, E.G. Kiyikci, Gasification of wood and torrefied wood with air, oxygen, and steam in a fixed-bed pilot plant, Energy & Fuels, 30 (2016) 4034–4043.

[27] A. Horvat, M. Kwapinska, G. Xue, L.P.L.M. Rabou, D.S. Pandey, W. Kwapinski, J.J. Leahy, Tars from fluidized bed gasification of raw and torrefied Miscanthus x giganteus, Energy & Fuels, (2016).

[28] J. Corella, M.P. Aznar, J. Gil, M.A. Caballero, Biomass gasification in fluidized bed: where to locate the dolomite to improve gasification?, Energy & Fuels, 13 (1999) 1122–1127.

[29] L. Garcia, M.L. Salvador, J. Arauzo, R. Bilbao, Influence of catalyst weight/biomass flow rate ratio on gas production in the catalytic pyrolysis of pine sawdust at low temperatures, Ind. Eng. Chem. Res., 37 (1998) 3812–3819.

[30] L. Garcia, M.L. Salvador, J. Arauzo, R. Bilbao, Catalytic steam gasification of pine sawdust. Effect of catalyst weight/biomass flow rate and steam/biomass ratios on gas production and composition, Energy & Fuels, 13 (1999) 851−859.

[31] L. García, M.L. Salvador, J. Arauzo, R. Bilbao, Catalytic pyrolysis of biomass: influence of the catalyst pretreatment on gas yields, Journal of Analytical and Applied Pyrolysis, 58–59 (2001) 491−501.

[32] L. Garcia, M.L. Salvador, R. Bilbao, J. Arauzo, Influence of calcination and reduction conditions on the catalyst performance in the pyrolysis process of biomass, Energy & Fuels, 12 (1998) 139–143.

[33] S. Rapagna, M. Virginie, K. Gallucci, C. Courson, M. Di Marcello, A. Kiennemann, P.U. Foscolo, Fe/olivine catalyst for biomass steam gasification: Preparation, characterization and testing at real process conditions, Catal. Today, 176 (2011) 163–168.

[34] J.N. Kuhn, Z. Zhao, A. Senefeld-Naber, L.G. Felix, R.B. Slimane, C.W. Choi, U.S. Ozkan, Ni-olivine catalysts prepared by thermal impregnation: Structure, steam reforming activity, and stability, Applied Catalysis A: General, 341 (2008) 43–49.

[35] J.N. Kuhn, Z.K. Zhao, L.G. Felix, R.B. Slimane, C.W. Choi, U.S. Ozkan, Olivine catalysts for methane- and tar-steam reforming, Appl. Catal. B-Environ., 81 (2008) 14–26.

[36] X. Huang, M.J. Beck, Metal-free low-temperature water–gas shift catalysis over small, hydroxylated ceria nanoparticles, ACS Catalysis, 5 (2015) 6362–6369.

[37] C. Christodoulou, D. Grimekis, K.D. Panopoulos, E.P. Pachatouridou, E.F. Iliopoulou, E. Kakaras, Comparing calcined and un-treated olivine as bed materials for tar reduction in fluidized bed gasification, Fuel Process. Technol., 124 (2014) 275–285.

[38] F. Kirnbauer, H. Hofbauer, The mechanism of bed material coating in dual fluidized bed biomass steam gasification plants and its impact on plant optimization, Powder Technology, 245 (2013) 94–104.

[39] C. Dueso, M. Ortiz, A. Abad, F. García-Labiano, L.F. de Diego, P. Gayán, J. Adánez, Reduction and oxidation kinetics of nickel-based oxygen-carriers for chemical-looping combustion and chemical-looping reforming, Chemical Engineering Journal, 188 (2012) 142–154.

[40] Z. Huang, F. He, K. Zhao, Y. Feng, A. Zheng, S. Chang, Z. Zhao, H. Li, Natural iron ore as an oxygen carrier for biomass chemical looping gasification in a fluidized bed reactor, Journal of Thermal Analysis and Calorimetry, 116 (2014) 1315–1324.

[41] T.L. Westover, M. Phanphanich, M.L. Clark, S.R. Rowe, S.E. Egan, A.H. Zacher, D. Santosa, Impact of thermal pretreatment on the fast pyrolysis conversion of southern pine, Biofuels, 4 (2012) 45–61.

[42] K.R. Gaston, M.W. Jarvis, P. Pepiot, K.M. Smith, W.J. Frederick, M.R. Nimlos, Biomass Pyrolysis and Gasification of Varying Particle Sizes in a Fluidized-Bed Reactor, Energy & Fuels, 25 (2011) 3747–3757.

[43] R.J. Evans, T.A. Milne, Molecular characterization of the pyrolysis of biomass. 1. Fundamentals, Energy & Fuels, 1 (1987) 123–137.

[44] D.L. Carpenter, S.P. Deutch, R.J. French, Quantitative measurement of Biomass gasifier tars using a molecular-beam mass spectrometer: Comparison with traditional impinger sampling, Energy and Fuels, 21 (2007) 3036–3043.

[45] B. Acharya, I. Sule, A. Dutta, A review on advances of torrefaction technologies for biomass processing, Biomass Conv. Bioref., 2 (2012) 349–369.

[46] T. Melkior, S. Jacob, G. Gerbaud, S. Hediger, L. Le Pape, L. Bonnefois, M. Bardet, NMR analysis of the transformation of wood constituents by torrefaction, Fuel, 92 (2012) 271–280.

[47] B. British Standards Institution, C. European Committe for Standardization, Biomass gasification : tar and particles in product gases : sampling and analysis, 2006.

[48] Q. Xu, S. Cheah, Y. Zhao, Initial reduction of the NiO(100) surface in hydrogen, The Journal of Chemical Physics, 139 (2013) 024704.

[49] D.L. Carpenter, R.L. Bain, R.E. Davis, A. Dutta, C.J. Feik, K.R. Gaston, W. Jablonski, S.D. Phillips, M.R. Nimlos, Pilot-Scale gasification of corn stover, switchgrass, wheat Straw, and wood: 1. Parametric study and comparison with literature, Ind. Eng. Chem. Res., 49 (2010) 1859–1871.

[50] J. Herguido, J. Corella, Gonzalez-Saiz, Steam gasification of lignocellulosic residues in a fluidized bed at a small pilot scale. Effect of the type of feedstock., Industrial and Engineering Chemistry Research, 31 (1992) 1274–1282.

[51] P. Pérez, P.M. Aznar, M.A. Caballero, J. Gil, J.A. Martín, J. Corella, Hot gas cleaning and upgrading with a calcined dolomite located downstream a biomass fluidized bed gasifier operating with steam-oxygen mixtures, Energy and Fuels, 11 (1997) 1194–1197.

[52] A.K. Stark, R.B. Bates, Z. Zhao, A.F. Ghoniem, Prediction and validation of major gas and tar species from a reactor network model of air-nlown fluidized bed biomass gasification, Energy & Fuels, 29 (2015) 2437–2452.

[53] R.B. Bates, C. Altantzis, A.F. Ghoniem, Modeling of biomass char gasification, combustion, and attrition kinetics in fluidized beds, Energy & Fuels, 30 (2016) 360–376.

[54] J.R. Rostrup-Nielsen, J. Sehested, J.K. Norskov, Hydrogen and synthesis gas by steam- and CO_2 reforming, Advances in Catalysis, Academic Press Inc, San Diego, 2002, pp. 65–139.

[55] A. Felix; Larry Gordon (Pelham, I. Rue; David M.(Chicago, T.P.E. Seward III, NY), L.E.L. Weast, IL) Method for producing catalytically active glass-ceramic materials, and glass-ceramics produced thereby in: USPTO (Ed.), Gas Technology Institute, USA, 2009.

[56] F. L., C. Choi, R. Slimane, G. Arkenberg, S. Swartz, J. Kuhn, U. Ozkan, Z. Zhao, Thermally impregnated Ni-olivine catalysts for decomposig tar in biomass gasification, 16th European Biomass Conference & ExhibitionValencia, Spain, 2008, pp. 499.

[57] M. Funaoka, T. Kako, I. Abe, Condensation of lignin during heating of wood, Wood Science and Technology, 24 (1990) 277–288.

[58] F. Kačík, J. Luptáková, P. Šmíra, A. Nasswettrová, D. Kačíková, V. Vacek, Chemical alterations of pine wood lignin during heat sterilization, BioResources, 11 (2016) 3442–3452.

[59] A.K. Starace, R.J. Evans, D.D. Lee, D.L. Carpenter, Effects of torrefaction temperature on pyrolysis vapors products of woody and herbaceous feedstocks, Energy & Fuels, 30 (2016) 5677–5683.

[60] A.M. Scheer, C. Mukarakate, D.J. Robichaud, G.B. Ellison, M.R. Nimlos, Radical chemistry in the thermal decomposition of anisole and deuterated anisoles: an Investigation of aromatic growth, Journal of Physical Chemistry A, 114 (2010) 9043–9056.

Biomass

Gasifier

Thermally-treated **Untreated**

Biomass feeder

Fluidized bed

Plain Olivine or Ni-Ce Olivine